LISM STRUCTURE – FRAGMENTED SUPERBUBBLE SHELL?

P. C. FRISCH
Univ. Chicago, Dept. Astronomy Astrophysics, 5640 S. Ellis Ave, Chicago, IL 60637, USA

Abstract. Small scale structure in local interstellar matter (LISM) is considered. Overall morphology of the local cloud complex is inferred from Ca II absorption lines and observations of H I in white dwarf stars. Clouds with column densities ranging from 2–100 $\times$ 10^{17} cm^{-2} are found within 20 pc of the Sun. Cold (50 K) dense ($\sim 10^5$ cm^{-3}) small (5–10 au) clouds could be embedded and currently undetected in the upwind gas. The Sun appears to be embedded in a filament of gas with thickness $\leq$0.7 pc, and cross-wise column density $\leq$ 2 $\times$ 10^{17} cm^{-2}. The local magnetic field direction is parallel to the filament, suggesting that the physical process causing the filamentation is MHD related. Enhanced abundances of refractory elements and LISM kinematics indicate outflowing gas from the Scorpius-Centaurus Association. The local flow vector and λ Sco data are consistent with a 4,000,000 year old superbubble shell at $\sim$–22 km s^{-1}, which is a shock front passing through preshock gas at $\sim$–12 km s^{-1}, and yielding cooled postshock gas at $\sim$–26 km s^{-1}in the upwind direction. A preshock magnetic field strength of 1.6 μG, and postshock field strength of 5.2 μG embedded in the superbubble shell, are consistent with the data.

Key words: Local Interstellar Medium, Superbubbles, Local Bubble models

Abbreviations: LISM – Local ISM; SIC – Surrounding Interstellar Cloud; LIC – Local Interstellar Cloud

1. Introduction

Small scale spatial structure in local interstellar matter ("LISM") increases the fraction of interstellar gas in cloud surface regions, and indicates inhomogeneous physical properties on subparsec scale sizes. Unresolved velocity differences between adjacent structures will mimic turbulence, and reduce the accuracy with which the velocity of the interstellar cloud surrounding the solar system can be inferred from observations of absorption lines in stars. The physical properties of the surrounding interstellar cloud ("SIC") are inferred from observations of stars distanced 1.3–200 pc from the Sun, whereas the heliopause is only $\sim$0.0005 pc distant. Therefore, sightline averaged cloud properties do not necessarily correspond to the physical properties of the interstellar cloud which surrounds the solar system.

Interstellar matter establishes the galactic environment of the Sun, and the solar wind regulates the interaction between the solar system and the SIC. Over the past 5-10 million years the solar system has traveled through a region of space relatively empty of interstellar clouds, with average densities less than 0.0002 cm^{-3} (Frisch & York, 1986). Within the past few hundred thousand years, the Sun encountered the interstellar cloud complex local to the Sun. At the SIC low densities, the solar wind effectively excludes interstellar gas from the 1 AU region containing the Earth. However, 10%–15% of diffuse ISM is contained in cold dense structures (T$\sim$50 K, n$\sim$ 6000 – 10^5 cm^{-3}) with scale sizes of 5 AU to 100 AU (Frail *et al.*, 1991). The

Space Science Reviews **78**: 213–222, 1996.

lowest column density seen for these structures is 9.3×10^{18} cm^{-2}. Evidently, if a density structure such as these were embedded in the upwind cloud, the heliopause radius would collapse to 1–2 au, strongly altering the 1 AU environment of the Earth.

These possibilities motivate a study of the small scale structure in local interstellar matter.

2. LISM Morphology

There are some salient asymmetries in the distribution of interstellar gas within 35 pc of the Sun. Figs. 1, 2 summarize the overall distribution of this gas, based on Ca II data towards 42 stars and N(H) data towards an additional 16 white dwarf stars. The average space density of H I in the LISM, n(H I)$\sim$ 0.1 cm^{-3}, is used to scale the overall morphology of the LISM. Since the ionization potential of Ca II is 6.1 eV, which is less than the 13.6 eV H I ionization potential, $\sim$10% of the LISM calcium is in the form Ca II ($\sim$90 % is Ca III). Observations towards η UMa give a LISM conversion factor N(Ca II)/N(H I+H II)$\sim 10^{-8}$, since N(H I+H II)=10^{18} cm^{-2} and N(Ca II)=10^{-8} cm^{-2} (Frisch & Welty, 1996). This same factor is found for α Oph, with log N(Ca II)=11.53 cm^{-2} (Crawford & Dunkin, 1995) and log N(H I)=19.48 cm^{-2} (Frisch, York, & Fowler, 1987). When all available data sampling the LISM are considered, N(Ca II)/N(H I+H II) varies by a factor of 10 between sightlines, as does N(Mg II)/N(H I+H II). N(Fe II)/N(H I+H II) varies locally by a factor of 5. Although Ca II is a trace element and sensitive to both density ($\sim n^2$) and abundance variations, the greater amount of data available on Ca II than either Mg II or Fe II make it a useful tracer of nearby LISM.

Using this scaling relation, the local cloud complex extends 3 parsecs towards η UMa, a star in the North Galactic Pole region, but 30 pc towards α Gru, a star near the South Galactic Pole region (Frisch & York, 1991). In the anti-center region the local cloud complex extends 3-5 pc, while in the galactic center region it extends $\sim$30 pc. Thus, the Sun is located closest to the "top" and anti-center portion of local cloud complex. This configuration is consistent with the structure determined from Mg II lines (Genova *et al.*, 1990). Figs. 1, 2 summarize the overall LISM morphology, based on Ca II absorption lines and the Ca II/H I=10^{-8} conversion factor, and white dwarf H I data.

3. Small Scale Structure

The LISM shows individual interstellar "clouds" with column densities N(H I)= $2 - 100 \times 10^{17}$ cm^{-2}. Clouds at the low end of this column density range will be masked in sightlines with larger column densities, unless the clouds are well separated in velocity. Structure in interstellar matter is seen as variations in interstellar

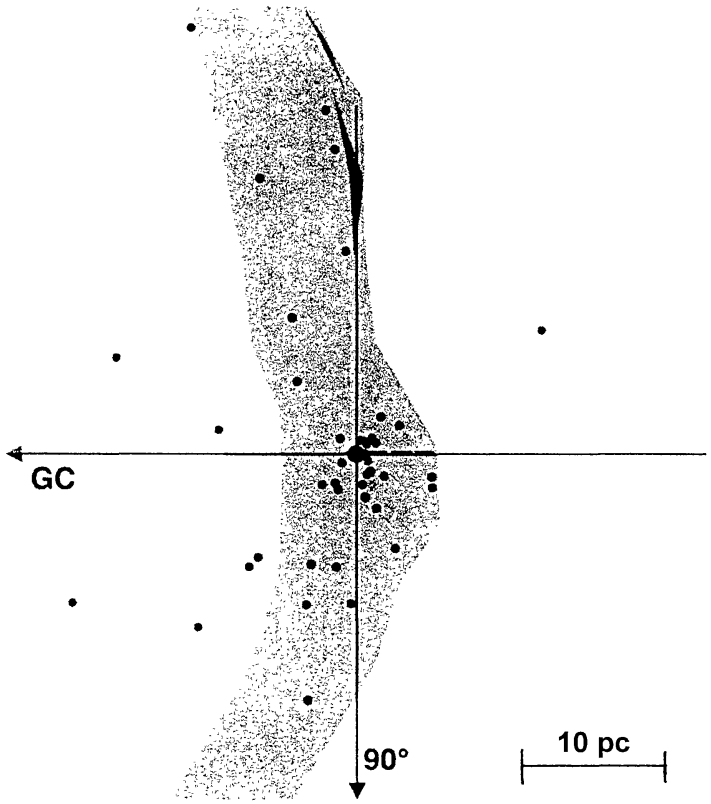

Figure 1. Overall distribution of interstellar gas within 30 pc of the Sun, based on observations of interstellar Ca II lines in 42 stars and observations of 16 white dwarf stars. The conversion factor N(Ca II)/N(H I+H II)$\sim 10^{-8}$ is used. The SIC was assumed to have an average density of 0.1 cm^{-3} for this plot. Data for stars with known circumstellar gas or peculiar emission lines are omitted. Data points with high excursions from the surface represent sightlines with denser clouds. The viewpoint is the north galactic pole.

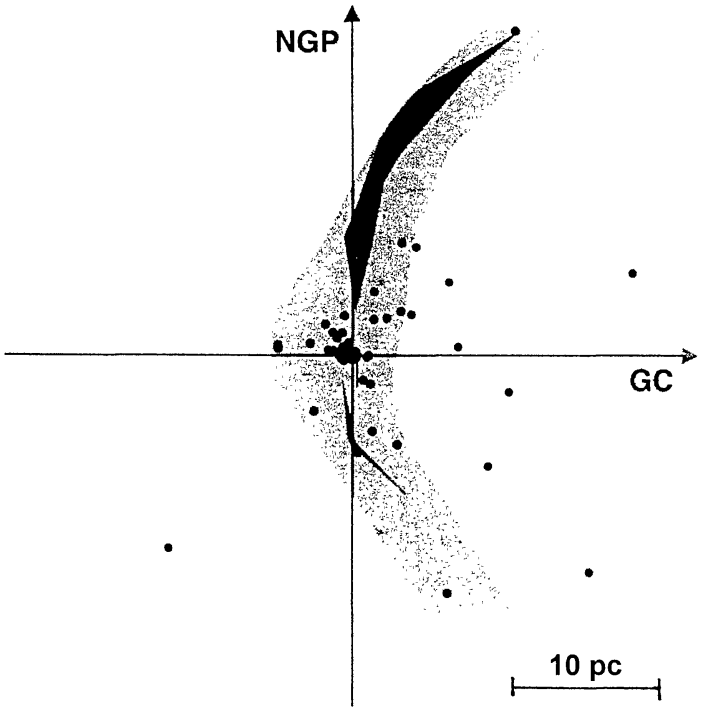

Figure 2. Same as Figure 1, but viewed from a longitude of 270°.

column densities over small angular scales (Munch & Unsold, 1962; Diamond *et al.*, 1995; Frail *et al.*, 1991; Meyer & Blades, 1996), and as spectrally resolved Doppler broadened interstellar absorption components. In the LISM, the galactic interval around the tangential sightline towards the Loop I supernova remnant bubble, l∼0°–30°, shows pronounced angular variation in Ca II column densities for stars within 20 pc: towards α Oph (l=36°, b=+23°, d=20 pc), log N(Ca II)=11.53 cm^{-2} (Crawford & Dunkin, 1995); whereas towards γ Oph (l=28°, b=+15°, d=29 pc), log N(Ca II)=10.86 cm^{-2}; and towards λ Aql (l=31°, b=–6°, d=30 pc), log N(Ca II)<9.59 cm^{-2} (Vallerga *et al.*, 1993). The interstellar gas in this region also shows a complex velocity structure: three Ca II absorption line components are seen towards α Aql (l=48°, b=–9°, d=5 pc), and log N(Ca II)=10.26 cm^{-2} (Bertin *et al.*, 1993). Typical minimum observed Ca II line strengths of 1 mÅ are seen in the LISM, corresponding to log N(H I)∼18.0 cm^{-2} clouds. Towards Sirius (2.7 pc), two absorption features are seen with column densities log N(H I)=17.23 cm^{-2} (Bertin *et al.*, 1995). At the 3.6 km sec^{-1} resolution of the Hubble Space Telescope GHRS, it is estimated that only 10% of the interstellar velocity components are resolved for unsaturated lines (Welty, Morton, & Hobbs, 1996). The range of column densities for cloud structures near the Sun is shown in Figure 3, where N(Ca II) is plotted versus galactic longitude for individual absorption components sampling ISM within 50 pc. Ultimately, high spectral resolution observations (∼0.4 km s^{-1}) in the ultraviolet region (1000-3000 Å) will be required to uniquely define the cloud structure in the LISM.

The presence of clouds with column densities ranging from 2-100 × 10^{17} cm^{-2} in the LISM makes it difficult to uniquely determine the SIC velocity, since clouds with 3 × 10^{17} cm^{-2} may be blended with higher column density features. This is certainly the case in the upwind direction where column densities exceed 10^{19} cm^{-2}. These uncertainties are shown by the fact that absorption components at the LIC * velocity are not found in the Fe II and Mg II lines towards α Cen (1.3 pc) (Lallement *et al.*, 1995). They are also not seen in the Ca II line towards η UMa, which has a very low column density (10^{18} cm^{-2}) (Frisch & Welty, 1996). Either the LIC velocity is not the velocity of the SIC, or in both cases the SIC cloud extent is very short in the sightline (≤0.6 pc). However, the heliocentric upwind direction is fixed by observations of SIC H I and He I in the solar system, so the SIC velocity would deviate from the LIC velocity vector in magnitude, rather than direction.

One interesting question is whether dense, low column density, cold clouds (n∼10^5 cm^{-3}, log N(H I)∼10^{19} cm^{-2}, T∼50 K, thickness ∼5–10 au) embedded in the upwind gas might have gone undetected? Typically, Ca II in cold diffuse interstellar clouds is depleted by a factor of 20 more than in LISM-type gas; thus the predicted Ca II column density associated with such a cloud would be log N(Ca II)=9.7 cm^{-2}. At 50 K, the Ca II Doppler constant is b= 0.14 km s^{-1}

* The "Local Interstellar Cloud" (LIC) is defined by the velocity vector of 25.7 km s^{-1} flowing from the direction l=5.9°, b=+16.7° (Lallement & Bertin, 1992). If the LIC velocity describes the velocity of the surrounding cloud, then the LIC is the SIC.

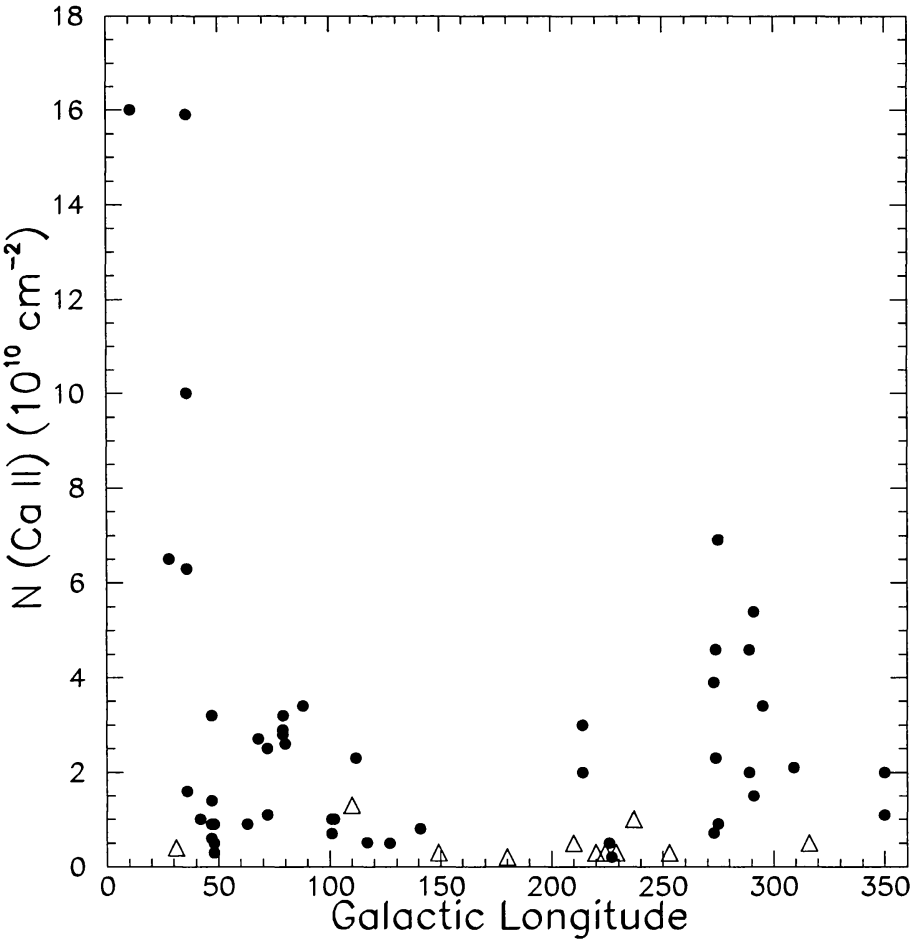

Figure 3. N(Ca II) is plotted versus galactic longitude for individual absorption components for stars sampling ISM within 50 pc. Stars in the "high Mg II column density" region of Genova *et al.* (1990) (viz. low galactic latitudes and the galactic center hemisphere, where log N(Mg II)> 12.1 cm^{-2}) are plotted as filled circles, while stars in low Mg II regions are plotted as open circles. Upper limits are plotted as open triangles. Data for stars with known circumstellar gas or peculiar emission lines are omitted.

(corresponding to a full-width-half-max of 0.2 km s^{-1}). Absorption from the cold gas would be weak, and contribute only 0.4 mÅ absorption to the Ca II 3933 Å line, and if blended in velocity with adjacent warm gas, it would *not* be resolved by existing observations. Therefore, one must conclude that dense small structures could be embedded in nearby upwind interstellar gas. If the ultraviolet Zn II line were available for a nearby star in the upwind direction, for instance, then it would be possible to determine if dense structures are present since depletion would not be a factor.

4. Structure of SIC

Given the evidence for clouds with column densities 2×10^{17} cm^{-2} in the LISM, the overall cloud morphology in Figs 1, 2 becomes the envelope of the distribution

of nearby interstellar gas. In order to construct the surrounding cloud structure, one may assume that the cloud is moving in a direction parallel to the cloud surface normal, and then use the component column density towards a nearby star to constrain the distance to the cloud surface in that direction. This assumption rests on the result that the kinematics of nearby interstellar matter (d<20 pc) is consistent with an expanding superbubble origin (Frisch, 1996). In this case, the LIC cloud column density towards the star Sirius led to the conclusion that the Sun has entered the LIC cloud within the last 2,000-8,000 years, and that the Sun is about ~0.1 pc from the surface in the downwind direction (Frisch, 1994). When the upper limits on the Ca II column density towards λ Aql (Vallerga *et al.*, 1993) and the LIC Fe II column density towards α Cen (Lallement *et al.*, 1995) are included, then we are forced to conclude that the Sun is located in a filament of diffuse interstellar gas with total thickness < 0.7 pc. This filament is illustrated in Figure 4, along with additional cloud structures representing cloud multiplicity seen towards nearby stars. If this picture is correct, however, then most of the interstellar gas observed towards α Aur, in the downwind direction, must be in separate, but co-moving, filaments (or clouds) from the surrounding cloud. The thickness of the SIC filament corresponds to a column density of $\sim 2 \times 10^{17}$ cm^{-2}. Filamentary structures are not unusual in interstellar gas; for instance they are seen where the Cygnus superbubble interacts with interstellar clouds (Graham *et al.*, 1995).

The LISM interstellar magnetic field direction traced by observations of polarization in the nearest stars (d=2–30 pc) is directed towards l~70°, and therefore is parallel to the SIC cloud surface. The polarization is within 3 pc of the Sun in the upwind direction, and there is little change with polarization strength as a function of star distance. Therefore, this magnetic field may be captured in the SIC filament. Alternately, the polarizing magnetic field could be captured in the higher column density, higher velocity gas within ~1 pc of the Sun in the upwind direction. Additional discussion of the Tinbergen polarization data can be found in Frisch (1991, 1996). The facts that the SIC properties are consistent with a filamentary structure, and that the local magnetic field is parallel to this filament, suggest to the author that the physical process causing the filamentation is linked to a cloud fragmenting due to instabilities. For SIC values n=0.15 cm^{-3}, T=7,000 K, estimated B=1.6 μG, the ratio of gas pressure to magnetic pressure, $\beta \sim 1$.

5. Superbubble

The kinematics and abundance patterns in local interstellar matter (LISM), combined with the large angle subtended by the Loop I supernova remnant, led to the view that the Sun is immersed in the shell of the Loop I remnant, associated with the Scorpius-Ophiuchus Association superbubble (Frisch, 1981, and see Breitschwerdt

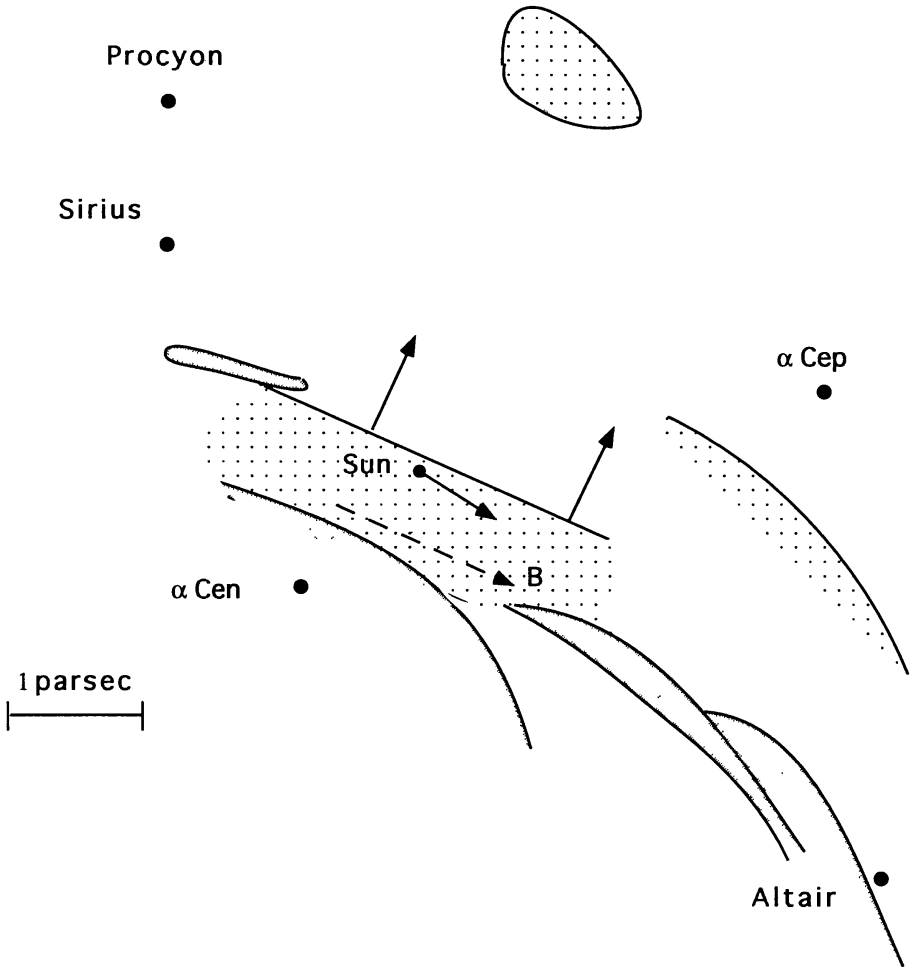

Figure 4. Morphology of the interstellar cloud surrounding the Sun, inferred by assuming that the cloud velocity vector is parallel to the surface normal (as would be expected for an expanding superbubble shell), and constrained by LIC column densities (or limits) observed towards Sirius, α Cen, and λ Aql (see text). Cloud multiplicity towards Sirius, α Cen, and Altair is also illustrated.

et al., this volume). The cloud surrounding the solar system has been modeled as part of a superbubble shell formed ~4,000,000 years ago around this association,

Looking first at the kinematics of the LISM gas: this gas flows past the Sun from an upwind direction (in the local standard of rest, LSR) directed at the Scorpius-Ophiuchus Association, but the flow is not uniform. The upwind velocity vector, after transforming into the LSR velocity frame, corresponds to V~–19, l~ 335°, b~ 0° (with the exact value dependent on the assumed flow vector and local standard of rest transformation). For the velocities of 24 interstellar components observed optically for stars within 50 pc of the Sun, the RMS variation from the local flow velocity vector is 2.4 km s^{-1}. In contrast, the RMS variation from the LSR for 23 component velocities is 6.5 km s^{-1}. Thus, it is possible to select a set of LISM clouds from a sample of nearby stars which give a relatively coherent flow at the local flow velocity, but it is not possible to select a set of components (from this

same sample of stars) which are at rest in the LSR. * In conclusion, the fit of the local flow velocity vector to the velocities of interstellar absorption components in nearby stars is significantly better than the fit of the LSR velocity. The dispersion shows, however, that the flow is not a uniform and linear. The velocity vector of the LISM establishes this gas as outflowing from the Scorpius-Centaurus Association.

The second characteristic indicating that the LISM gas has been processed through a shock front is the anomalously high gas abundance pattern seen in this material. For the LISM clouds, typically N(Ca II)/N(H I+H II)=10^{-8}. The enhanced abundance of refractories appears to be a global property of interstellar matter within 20-30 pc of the Sun, since it is found towards both α Oph, with log N(H I)=19.48 cm^{-2} (Frisch, York, & Fowler, 1987), and towards η UMa, with log N(H I+H II)=18.00 cm^{-2} (Frisch & York, 1991)). In contrast, the ratio 4.8×10^{-10} is found towards the cold cloud complex in ζ Oph. The enhanced abundance pattern of refractory elements is also seen for the elements Ti II, Fe II and Mg II in the LISM. IUE satellite data show that Fe II and Mg II are depleted towards η UMa by factors of 9 and 12, respectively. Better quality Hubble data show average depletions for the LIC components in α CMa, α CMi, α Aur, ϵ CMa of a factor of 6 for Fe II, and a factor of 11 for Mg II. These depletions can be contrasted by the ζ Oph cold cloud depletion of a factor of 275 for Fe II, for example, and about 25 for Mg II (after correcting the λ1240 line pair oscillator strengths upwards by a factor of 3, Welty, private communication).

In the superbubble scenario, the LISM is gas evaporated from the surfaces of molecular clouds embedded in the Scorpius-Ophiuchus Association during earlier and more active periods (much as the clouds embedded in the Cygnus Loop superbubble are currently evaporating due to interactions with blast waves, (Graham *et al.*, 1995)). The characteristics of the upstream gas are consistent with a superbubble shell formed 4,000,000 years ago, with radius 160 pc and local standard of rest velocity 22.4 km s^{-1}(corresponding to the upwind gas velocity), expanding into a cloud of density n$\sim$0.1 cm^{-3} (Frisch, 1995), but this simple shell model neglects magnetic fields which would be significant. The shell is a "fossil superbubble shell", and unless grain-grain collisions are effective, grain destruction would not be taking place currently at this relatively low cloud velocity. Superbubble shell velocities are given by V$\sim$$age^{-0.4}$, so the grain destruction would have taken place either during the cloud evaporation or within about 10,000 years after the shell formed initially. The enhanced LISM abundances could be due to dust grain destruction at earlier epochs when the shell velocity exceeded $\sim$100 km $s^{-1}$and grain mantle destruction via sputtering would have been effective (e. g. see Draine, 1995).

Building on the view that the nearest interstellar gas has been processed through a shock front, cloud components seen by the Copernicus satellite towards the low column density star λ Sco (l=372°, b=–2°, d=85 pc) have been interpreted in

* For each star, where more than one component is present, the component used for the calculation was selected so as to minimize the chosen variation. The measurement uncertainties typically are 2-3 km s^{-1}. See Frisch (1996) for additional information.

terms of a shock front moving through the gas (Frisch & York, 1991). The Ca II component heliocentric velocities seen towards this star are at –26.6 km s^{-1} and -19.1 km s^{-1} (Welty, Morton, & Hobbs, 1996), which convert to LSR velocities -19.6 km s^{-1} and -12.1 km s^{-1} The rest of the velocities quoted in this paragraph are in the LSR velocity frame. For an adiabatic shock in a perfect gas, with no magnetic field, the two components observed optically in λ Sco correspond to the preshock and postshock gas. In this model, the preshock gas was identified as the cloud at –12.1 km s^{-1} (York, 1993, found this cloud to be mainly ionized), and the postshock gas was identified as the mainly neutral thin sheet of gas at –19.6 km s^{-1} cloud. The shock front was identified as the gas at –22 km s^{-1} These clouds are upwind of the Sun. A more detailed discussion of this model can be found in Frisch and York 1991).

An adiabatic shock model can also be fit to the data towards α Oph, using Ca II velocities (Crawford & Dunkin, 1995). In this direction, the shock front would be the -14 km s^{-1} (LSR velocities) component, the preshock and postshock gas would correspond to the –5.6 km $s^{-1}$and –8.2 km s^{-1} components.

For both sightlines, magnetic fields are present since the superbubble shell appears to be threaded by a magnetic field. Based on Zeeman splitting observations in other sightlines through the Loop I superbubble, the magnetic field in the postshock gas is estimated at <B>=–5.2 μG, which would give a preshock value of <B>=–1.3 μG (Frisch & York, 1991). These fields would modify the simple shock approximations used for this shock model, and this question needs to be considered in more detail.

6. Conclusions

In this review, the overall morphology of the LISM gas is inferred from interstellar Ca II absorption lines and observations of H I in white dwarf stars. Clouds with column densities ranging from 2–300 $\times$ 10^{17} cm^{-2} are found within 20 pc of the Sun. Because of the increased depletion in cold clouds, cold (50 K) dense ($\sim 10^5$ cm^{-3}) small (5–10 au) clouds could be embedded undetected in the upwind gas. The factor of 10 variation found in the LISM Ca II and Mg II abundances, and factor of 5 seen in the LISM Fe II abundance, indicate density variations must be present. These structures require ultraviolet data of lines such as Zn II in order to be detected. With simple assumptions, one concludes that the Sun is embedded in a filament of gas with thickness $\leq$0.7 pc, and cross-wise column density $\leq 2 \times 10^{17}$ cm^{-2}; the local magnetic field appears to be parallel to the filament suggesting that the physical process causing the filamentation may be MHD related. Enhanced abundances of refractory elements, combined with the flow direction of local gas, indicate an origin associated with the Scorpius-Centaurus Association. A simple picture consistent with the data towards λ Sco is found if a 4,000,000 year old superbubble shell at $\sim$–22 km s^{-2} is a shock front passing through preshock gas at $\sim$–12 km s^{-2} which

is ionized (or partially ionized), giving cooler and denser postshock gas at $\sim$–26 km s^{-2} in the upwind direction (LSR velocities). The preshock magnetic field would be 1.6 μG, and the postshock magnetic field, embedded in the superbubble shell, would be –5.2 μG. However, since a simple adiabatic shock model was considered, which should not apply to an old superbubble shell, this problem needs to be looked at in more detail.

Acknowledgements

I would like to thank the National Aeronautics and Space Administration for research support.

References

Bertin, P., Lallement, R., Ferlet, R., and Vidal-Madjar, A. 1993, Astronomy and Astrophysics, **278**, 549

Bertin, P., Vidal-Madjar, A., Lallement, R., Ferlet, R., and Lemoine, M., 1995, Astronomy and Astrophysics, **302**, 889

Crawford, I. A., Dunkin, S. K., 1995, Monthly Notices of the RAS, **273**, 219.

Diamond, C. J., Jewell, S. J., Ponman, T. J.: 1995, Monthly Notices of the RAS, **274** 589.

Draine, B. T., 1991, Astroph. Sp. Sci., **233**, 111

Frisch, P. C.: 1981, Nature, **293**, 377

Frisch, P. C.: 1991, in *COSPAR Colloquia Series, No. 1, Physics of the Outer Heliosphere*, S. Grzedzielski and E. Page (eds), (London: Pergamon), p. 19.

Frisch, P. C.: 1994, Science, **265**, 1423

Frisch, P. C.: 1995, Space Science Reviews, **72**, 499

Frisch, P. C., and Welty, D. E., 1996, in preparation.

Frisch, P. C., York, D. G.: 1986, in R. Smoluchowski, J. N. Bahcall, M. Matthews (eds.), *The Galaxy and the Solar System*, (Tucson: Univ. Arizona Press) pp. 83

Frisch, P. C.: 1996, *Cosmic Winds and the Heliosphere,* Jokipii, J. R., Sonett, C. P., Giampapa, M. S. (eds.), (Tucson: U. Arizona).

Frisch, P. C., York, D. G., and Fowler, J. R., 1987, Astrophysical Journal, **320**, 842

Frisch, P. C., York, D. G., 1991, in *Extreme Ultraviolet Astronomy,* R.F. Malina and S. Bowyer (eds.), (New York: Pergamon), p. 322

Genova, R., Molaro, P., Vladilo, G., and Beckman, J. E. 1990, Astrophysical Journal, **355,** 150.

Graham, J. R., Levenson, N. A., Hester, J. J., Raymond, J. C., and Petre, R., 1995, Astrophysical Journal, **444**, 787

Lallement, R., Bertin, P.: 1992, Astronomy and Astrophysics, **266**, 479

Frail, D. A., Weisberg, J. M., Cordes, J. M., Mathers, C.: 1994, Astrophysical Journal, **436,** 144.

Lallement, R., Ferlet, R., Lagrange, A. M., Lemoine, M., and Vidal-Madjar, A. 1995, Astronomy and Astrophysics, **304**, 461

Meyer, D. M., and Blades, J. C., 1996, Astrophysical Journal, **464,** 179L.

Munch, G. and Unsold, A., 1962, Astrophysical Journal, **135,** 711. 1994, Astrophysical Journal, **436,** 144.

Slavin, J.D., 1989, Astrophysical Journal, **346,** 718.

Welty, D. E., Morton, D. C., and Hobbs, L. M., 1996, Astrophysical Journal, in press.

Vallerga, J. V., Vedder, P. W., Craig, N., and Welsh, B. Y., 1993, Astrophysical Journal, **411,** 729

York, D. G., 1983, Astrophysical Journal, **264,** 172